



ISSN: 2617-6548

URL: www.ijirss.com

Snow avalanche mapping using sentinel-1 SAR change detection

 Daniker Chepashev¹,  Natalya Denissova²,  Olga Petrova³,  Gulzhan Daumova³,  Aigerim Kalybekova^{1,4*}

¹*Institute of Ionosphere, Almaty 050000, Kazakhstan.*

²*Department of Information Technology, D. Serikbayev East Kazakhstan Technical University, Ust-Kamenogorsk 070000, Kazakhstan.*

³*School of Earth Sciences, D. Serikbayev East Kazakhstan Technical University, Ust-Kamenogorsk 070000, Kazakhstan.*

⁴*Department of Mechanics, al-Farabi Kazakh National University, Almaty, 050040, Kazakhstan.*

Corresponding author: Aigerim Kalybekova (Email: aigerimkalybekova8@gmail.com)

Abstract

Snow avalanches pose a persistent threat to mountain communities, yet systematic inventories remain scarce where cloud cover and rugged topography limit optical remote sensing. Leveraging the all-weather capability of C-band radar, we design an automated workflow that transforms Sentinel-1 imagery into a season-scale avalanche record for the Zailiysky Alatau range (Northern Tien Shan, Kazakhstan). A dual-polarization Interferometric-Wide pair acquired in March–April 2024 was co-registered in Google Earth Engine, speckle-suppressed with an adaptive Enhanced Lee filter, and converted to a VV–VH polarization-difference layer. Temporal differencing highlighted fresh debris as negative anomalies. Layover, radar shadow, and permanent water were masked using the 30 m SRTM DEM and the JRC Global Surface Water product. Further, decision tree classifiers were used for delineation of avalanche from non-avalanche pixels. Validation against PlanetScope (3 m) and Sentinel-2 (10 m) imagery acquired within ± 2 days returned a detection completeness. Results confirm that Sentinel-1 change detection can retrieve most medium-to-large avalanches even under persistent cloud cover, offering a cost-free complement to sparse field observations in Central Asia. The workflow fully implemented in a cloud platform requires no scene-specific tuning and is transferable to other snow-covered mountain regions for near-real-time hazard assessment.

Keywords: Change detection, Decision-tree classification, Sentinel-1 SAR, Snow avalanche.

DOI: 10.53894/ijirss.v8i6.9947

Funding: This research is funded by the Committee of Science of the Ministry of Science and Higher Education of the Republic of Kazakhstan (Grant No. BR21882022 "Research of avalanche activity in the East Kazakhstan region for development of monitoring systems and scientific substantiation of their placement").

History: Received: 9 June 2025 / Revised: 14 July 2025 / Accepted: 16 July 2025 / Published: 18 September 2025

Copyright: © 2025 by the authors. This article is an open access article distributed under the terms and conditions of the Creative Commons Attribution (CC BY) license (<https://creativecommons.org/licenses/by/4.0/>).

Competing Interests: The authors declare that they have no competing interests.

Authors' Contributions: All authors contributed equally to the conception and design of the study. All authors have read and agreed to the published version of the manuscript.

Transparency: The authors confirm that the manuscript is an honest, accurate, and transparent account of the study; that no vital features of the study have been omitted; and that any discrepancies from the study as planned have been explained. This study followed all ethical practices during writing.

Acknowledgments: We are grateful to all the authors of the articles that were discussed in this review.

Publisher: Innovative Research Publishing

1. Introduction

Over the last few decades, intensified anthropogenic activities have accelerated global warming and climate change, which have resulted in increasingly frequent and severe extreme weather events [1]. These include abrupt and unexpected temperature and precipitation events, particularly rainfall and snowfall, which have the potential to trigger various disasters, such as landslides and snow avalanches [2]. Snow avalanches are catastrophic natural events in mountain regions characterized by the abrupt release of snow, ice, and occasionally rocks, soil, and plants that flow swiftly downhill [3]. They occur predominantly in mountainous terrain with steep topography and are triggered by a complex interaction of meteorological factors such as heavy snowfall, rapid warming, and rainfall, alongside terrain characteristics like slope angle, aspect, and surface roughness [2, 4]. They usually develop during or after major snowfall events, when the accumulation of snow exceeds the stability threshold of the snowpack, or during periods of rapid snowmelt, which reduces snowpack cohesion. A significant mass of snow breaks away and slides down the slope as a result of this accumulation destabilizing the snowpack. However, low in frequency, avalanches are difficult to predict, which can be dangerous and disruptive, causing serious damage to infrastructure, posing risks to human lives, and disrupting economic activities [5].

Different approaches have been developed for snow avalanche detection, including field surveys, aerial photography, and remote sensing techniques [6]. Field-based methods to measure avalanche activity include direct observation of avalanche paths, snow pit analysis, and the installation of sensors to detect ground vibrations or infrasound [7]. However, these techniques are often limited by accessibility, time constraints, and safety concerns in hazardous mountain environments. Weather conditions and the risk of triggering additional avalanches often make it difficult to access avalanche-prone areas. This results in substantial uncertainties and gaps in spatio-temporal mapping of avalanche activity, hampering effective risk assessment and mitigation efforts [8]. Therefore, aerial and satellite-based remote sensing techniques provide a synoptic, cost-effective, and timely approach for monitoring avalanches over large and inaccessible areas [9].

The adoption of remote sensing technologies not only facilitates the identification and monitoring of avalanches in extensive areas but also provides insights into the broader geological environment through sophisticated imaging and analysis techniques. These techniques can be crucial for identifying geological and topographical characteristics that influence the behavior of avalanches, such as slope angle, aspect, and surface roughness, which are pivotal in predicting avalanche risk [10]. The use of remote sensing in assessing slope stability and potential hazards is well-documented, demonstrating its effectiveness in environments where traditional methods are impractical due to safety or logistical constraints [11, 12]. In essence, remote sensing technologies offer a safer, more efficient way to collect comprehensive data, which is invaluable for studying avalanches and developing effective slope monitoring and risk management programs [13, 14].

Remote sensing imagery, particularly high-resolution multispectral data collected from aerial platforms and satellites such as Landsat, WorldView, QuickBird, and Sentinel-2, has been widely used for surveying otherwise inaccessible mountain terrain and mapping avalanche occurrences [6]. Recent advancements have resulted in the successful identification of avalanche occurrences and mapping debris extent using simple visual interpretation, object-based image classification, change detection techniques, and machine learning algorithms [15, 16]. These methods exploit the distinctive morphology, texture, and spectral signatures of avalanche deposits to differentiate them from the surrounding terrain, which helps in flagging high-risk areas [17]. However, the application of optical sensors and their performance is greatly sensitive to cloud cover, terrain shadow, and illumination conditions, which are prevalent in mountainous regions, especially during periods of heavy snowfall and reduced visibility. These limitations are further aggravated by the limited availability of high-resolution scenes, which are restricted to specific swaths, constraining rapid responses.

Radar-based remote sensing technologies offer a solution to overcome the limitations of optical imagery by providing continuous monitoring capabilities irrespective of weather conditions and solar illumination [18]. Synthetic Aperture Radar (SAR) sensors use microwave radiation to actively illuminate the Earth's surface and record the backscattered signal. SAR possesses unique advantages over optical sensors, particularly its ability to penetrate clouds and operate independently of solar illumination, making it suitable for avalanche monitoring in challenging weather conditions. Recent introduction of open-source satellite missions, like the European Space Agency's Sentinel-1 mission, offers new opportunities for avalanche monitoring with increased spatial and temporal resolutions. Avalanche mapping using Sentinel-1 SAR imagery relies on detecting changes in surface roughness and dielectric properties caused by avalanche events [17]. Changes in radar backscatter intensity and coherence between SAR images acquired before and after an avalanche event can be used to delineate avalanche deposits and track avalanche extent. Various studies have shown the effectiveness of change detection techniques for mapping snow avalanches using SAR data, demonstrating their potential for operational avalanche monitoring and risk management [15, 16, 19, 20].

The Northern Tien Shan mountain range is characterized by steep slopes, heavy snowfall, and frequent avalanche activity, making it a high-risk region for avalanches. The region experiences significant snowfall throughout the winter months, leading to the development of unstable snowpacks on steep slopes. Cloud cover associated with these storms often obscures the ground surface, which makes optical remote sensing data difficult to obtain [21]. SAR's all-weather imaging capabilities are especially valuable for timely detection and monitoring in such environments [22]. Therefore, the Northern Tien Shan provides an ideal case study to test and demonstrate the capabilities of Sentinel-1 SAR change detection for avalanche mapping. Moreover, the absence of systematic avalanche monitoring on the Kazakhstan side of the Northern Tien Shan mountain range highlights the need for remote sensing-based solutions to support avalanche risk management and mitigation efforts in the region. Thus, we have developed an automated workflow for detecting and delineating snow-avalanche occurrences in the Zailiysky Alatau range (Northern Tien Shan, Kazakhstan) using Sentinel-1 SAR data.

Furthermore, these results were validated through the visual representation of high-resolution PlanetScope and Sentinel-2 optical imagery, quantifying detection completeness and positional accuracy.

2. Study Area

Zailiysky Alatau is a mountain range in the northwestern Tien Shan mountains. It extends for 360 km with altitudes ranging from 1,300 to 4,973 meters above sea level [23]. Located in the south-eastern part of Kazakhstan (Figure 1), the northern slope of the mountain range borders with the city of Almaty [24]. The geographical location and high altitude of the region contribute to a continental climate characterized by cold winters and relatively mild summers. This powerful, snow-capped range stretches approximately 300 km from west to east, with a width of 40 km. The highest peaks in this mountain range can reach elevations of 4,500–5,000 meters above sea level, with an average elevation of about 4,000 meters. The region experiences significant snowfall during the winter months, with snow cover typically lasting from November to April or May [25]. As a result, snow avalanches are a common occurrence in the Zailiysky Alatau, posing a significant threat to infrastructure, transportation routes, and human settlements in the surrounding valleys [24]. The avalanche hazard season generally spans from November to April, with the highest frequency of avalanches occurring between March and April. These months coincide with maximum snowpack accumulation and rising temperatures, creating optimal conditions for avalanche formation. Thus, it becomes extremely important to analyze and map the avalanche-prone regions in the mountain range for risk assessment and mitigation management.

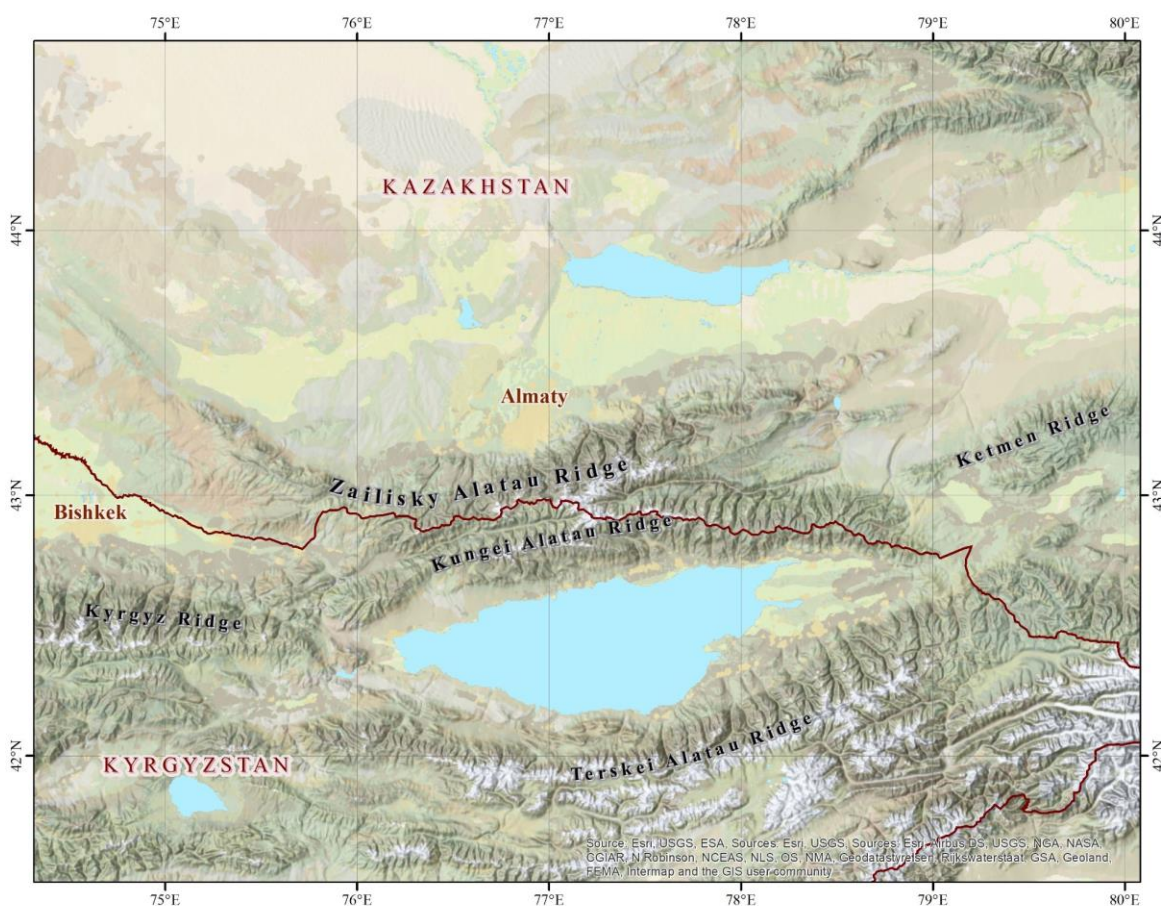


Figure 1.
Study area of the Zailiysky Alatau with the ridges.

3. Datasets and Methods

We deployed a comprehensive approach that combines Sentinel-1 SAR data processing, change detection techniques, and validation with high-resolution optical imagery to map snow avalanches in the Northern Tien Shan. Our approach leverages the unique capabilities of SAR sensors to overcome the limitations of optical imagery in cloudy and mountainous regions, providing a robust and reliable method for avalanche monitoring. Figure 2 illustrates the workflow used to process the imagery to automatically detect the changes in the snow cover due to avalanches. The methodology includes the following steps: data acquisition and preprocessing, change detection analysis, post-processing and refinement, and validation with optical imagery.

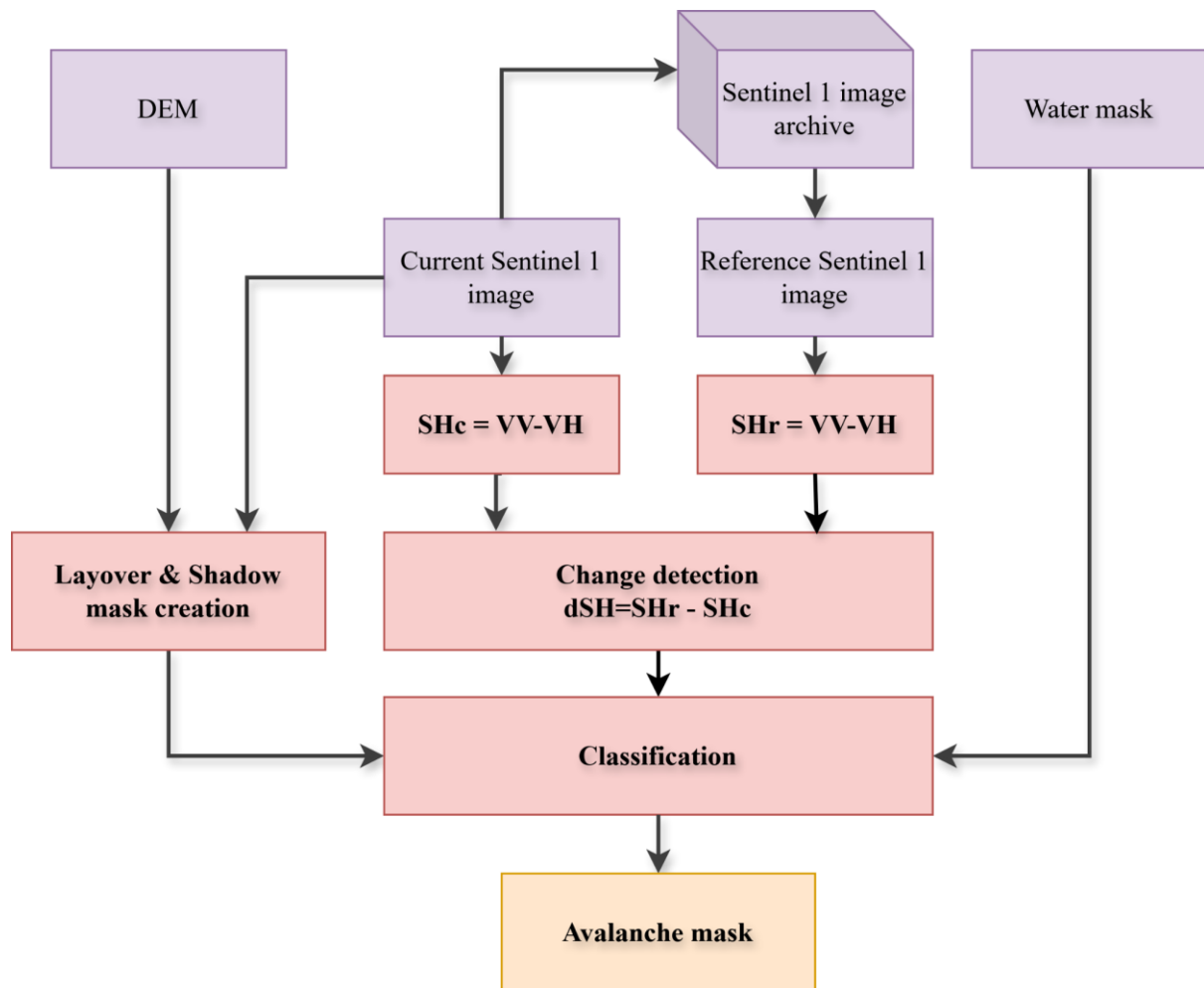


Figure 2.
The technical flowchart of the methodological approach for avalanche mapping.

3.1. Data Acquisition

The effectiveness of change detection techniques for mapping snow avalanches using SAR data has been demonstrated for operational avalanche monitoring and risk management [26]. The Sentinel-1 mission provides open-access C-band SAR data at a high spatial resolution (10m) and temporal resolution (6 days), making it suitable for monitoring changes in snow cover caused by avalanche events. The Sentinel-1 mission consists of two polar-orbiting satellites, Sentinel-1A and Sentinel-1B, which acquire SAR data in various modes and polarizations. We acquired Sentinel-1 Ground Range Detected (GRD) data from the COPERNICUS/S1_GRD collection using the Google Earth Engine data catalog. This dataset provides preprocessed images, which are already orthorectified, radiometrically calibrated, and terrain corrected. The preprocessed GRD datasets available in GEE provide pixel values in the form of backscatter intensity expressed in decibels (dB). The data was collected for the months of March and April 2024, encompassing the peak avalanche period in the Northern Tien Shan. This yielded dual-polarization (VV, VH) scenes acquired in Interferometric Wide Swath mode, which includes VV (vertical transmit/vertical receive) and VH (vertical transmit/horizontal receive) polarization bands.

For each “current” scene within this window, a “reference” scene possessing identical imaging geometry, same relative orbit, pass direction, and slice ID was selected to minimize layover- and shadow-related discrepancies that plague side-looking radar in steep terrain. The reference scenes were selected based on their proximity to the current scene, but always preceding it. Each image pair was then split into its VV and VH channels, from which we computed a VV – VH polarisation-difference index.

$$DI = \sigma_{VV}^0 - \sigma_{VH}^0 \quad (1)$$

Where, σ_0 denotes backscatter in decibels. Because VV and VH backscatter respond differently to surface roughness, the VV – VH polarization difference can provide enhanced sensitivity to subtle changes in surface conditions, such as those produced by avalanches disturbing the snowpack. The resulting difference layer (Figure 3) provides a comprehensive picture of the characteristics of the monitoring area at a given time.

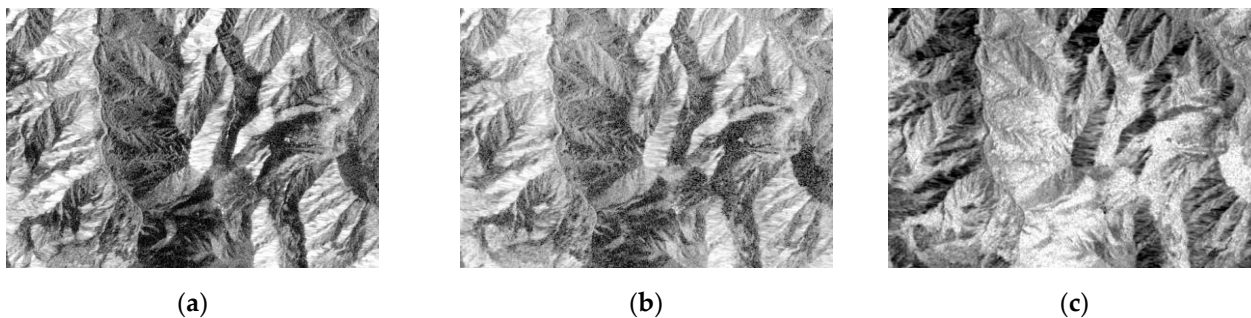


Figure 3. (a) VV polarization; (b) VH polarization; (c) difference between VV and VH polarization of Sentinel 1 image for the territory of Zailisky Alatau for April 18, 2024.

For applying the shadow mask and layover, the study utilized the Shuttle Radar Topography Mission Digital Elevation Model, available with a resolution of 1 arc-second (approximately 30m). Furthermore, the Global Surface Water dataset developed by the European Commission's Joint Research Centre was used to mask out water bodies. This collection offers statistics on the extent and change of various water surfaces as well as maps showing the location and temporal distribution of surface water [27]. All rasters were projected to UTM Zone 43 N (EPSG 32643) and resampled to 30 m, the working resolution of the inventory.

Furthermore, to validate the SAR-derived polygons, we used cloud-free optical scenes obtained within ± 2 days of the Sentinel-1 acquisitions from the PlanetScope and Sentinel-2 missions. PlanetScope imagery provides high-resolution (3-5 m) optical data with a high revisit frequency, allowing for detailed visual inspection of avalanche deposits and verification of the SAR-derived avalanche polygons. Sentinel-2 is a multispectral imaging mission that collects optical data in 13 spectral bands, including visible, near-infrared, and shortwave infrared [28]. With a spatial resolution of 10 meters, Sentinel-2 data products provide valuable information for characterizing snow cover and surface features. False-color composites (Blue-Green-NIR) enhance avalanche debris visibility. Thus, we used Sentinel-2 and PlanetScope data to corroborate avalanche classifications obtained from Sentinel-1 analysis.

3.2. Change Detection

SAR sensors emit microwave radiation and measure the backscattered signal from the Earth's surface, which is sensitive to changes in surface roughness, moisture content, and dielectric properties. The backscatter intensity is influenced by various factors, including the sensor's incidence angle, polarization, and the target's physical properties. By comparing SAR images acquired at different times, we can detect changes in backscatter intensity that may indicate the occurrence of snow avalanches [29]. We employed a multi-step approach to detect changes in backscatter intensity and identify potential avalanche locations [30]. Firstly, we performed image co-registration to ensure accurate pixel-to-pixel correspondence between the reference and current images.

We utilized the Enhanced Lee Filter available in the Sentinel Application Platform, with an adaptive window of (3x3 to 7x7 pixels) to reduce speckle noise while preserving the sharpness of the image [31]. The size of the filter window was adapted in accordance with local terrain roughness. Subsequently, we calculated the backscatter difference between the reference and current images for both VV and VH polarizations. This difference highlights areas where significant changes have occurred in surface roughness or dielectric properties, which may indicate the presence of avalanche debris. Negative difference values flag areas where surface roughness has increased, our primary signature of fresh avalanche deposits. Positive values mostly reflect illumination changes or snow ablation and are discarded in later masking and thresholding stages. The resulting rasters provide a noise-reduced, co-registered measure of backscatter change that feeds directly into the masking and decision-tree segmentation steps for further analysis.

3.3. Layover & Shadow Mas

Radar systems are affected by geometric distortions such as layover and shadow in areas with steep terrain. Layover occurs when the radar signal reaches the top of a mountain before it reaches the base, causing the top of the mountain to appear displaced towards the radar sensor. Shadowing occurs when the radar signal is blocked by terrain features, resulting in areas with no data. This is particularly pronounced in areas characterized by rugged topography, such as the Northern Tien Shan. To mitigate the effects of layover and shadow, we generated mask layers using the Shuttle Radar Topography Mission Digital Elevation Model [32]. The masks were derived using the orbital parameters of the Sentinel-1 constellation and the local incidence angle [9]. Layover and shadow areas (Figure 4) were excluded from the analysis to prevent false positives in avalanche detection.

Further, the JRC Global Surface Water mask was also applied to exclude water bodies from the analysis, as changes in water levels or ice cover can also cause changes in backscatter intensity that could be mistaken for avalanches [33]. Pixels flagged here were removed from the difference raster prior to the next change detection step, removing possible confounds from dynamic water bodies. By removing these areas, we focus the change detection analysis solely on terrain susceptible to snow avalanches, improving the accuracy of the results. By employing these masking techniques, we minimized the impact of geometric distortions and non-avalanche-related changes in backscatter intensity, thereby enhancing the accuracy and reliability of our avalanche detection results [34].

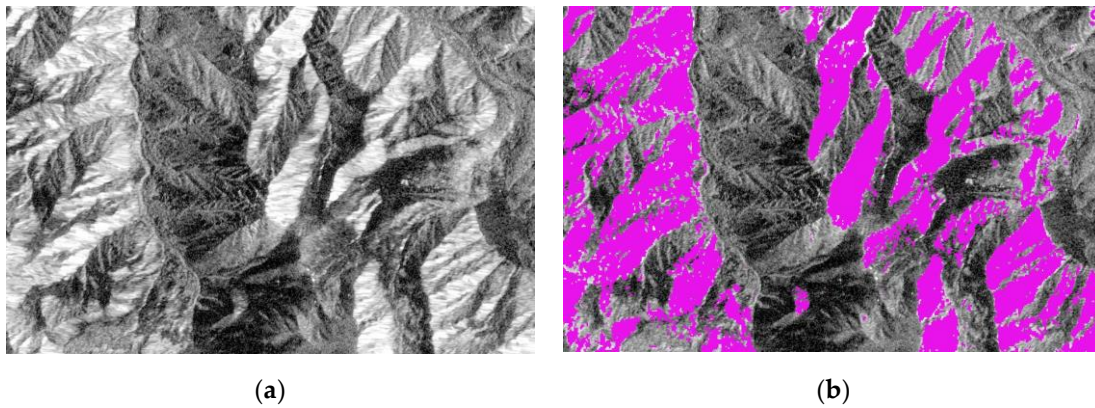


Figure 4.
Radar shadow and layover mask.

To transform the backscatter difference raster into discrete avalanche polygons, we employed a decision-tree segmentation approach based on backscatter thresholds [35]. The decision tree uses a set of predefined rules based on backscatter difference values, slope, and elevation to classify pixels as either avalanche or non-avalanche. First, we applied a threshold to the backscatter difference raster to identify potential avalanche pixels. This involved setting thresholds for the backscatter difference values above which a change is classified as an avalanche. The threshold values were determined based on the statistical distribution of backscatter differences in areas known to have experienced avalanches. For regions exhibiting significant topographic variability, we derived slope and aspect from the DEM to refine the classification process. These terrain attributes were used to create additional rules in the decision tree, helping to differentiate between avalanche-prone areas and areas where changes in backscatter intensity may be due to other factors.

After applying the thresholds and terrain-based rules, we performed a connected component analysis to group adjacent avalanche pixels into individual avalanche polygons. This involved identifying and delineating contiguous regions of avalanche pixels, which were then treated as individual avalanche events. Finally, the resulting avalanche polygons were subjected to a series of filtering and validation steps to remove false positives and ensure the accuracy of the results. This involved visual inspection of the polygons using high-resolution optical imagery (PlanetScope & Sentinel-2), as well as comparison with known avalanche occurrences or historical records. The method can objectively, accurately, and robustly detect regional automatic avalanches [36]. The validation of our avalanche mapping results is crucial for assessing the accuracy and reliability of the Sentinel-1 SAR change detection method [26].

4. Results and Discussion

The Sentinel-1 SAR change detection method has proven effective in mapping snow avalanches in the Northern Tien Shan, providing a valuable tool for monitoring and mitigating avalanche risks in remote and inaccessible regions. SAR's capacity to penetrate cloud cover and its sensitivity to changes in surface roughness enable consistent data acquisition regardless of weather conditions [37]. To illustrate the detection capabilities of our approach, a pair of Sentinel-1 images of the Zailiysky Alatau region near Big Almaty Lake was selected, processed, and analyzed for changes in backscatter intensity. Reference image from March 25, 2024 (Figure 5a) and the current image of April 18, 2024 (Figure 5b) were selected as they captured a period of significant avalanche activity in the region, characterized by heavy snowfall and subsequent warming trends. For each image, a difference index of VV and VH polarizations was calculated. On the resulting raster (Figure 5c), obtained using the image-algebra-based change detection algorithm, zones with minimal values, corresponding to the avalanche debris class, are clearly visible. It is found that the new avalanche deposits and their boundaries are clear in the difference image.

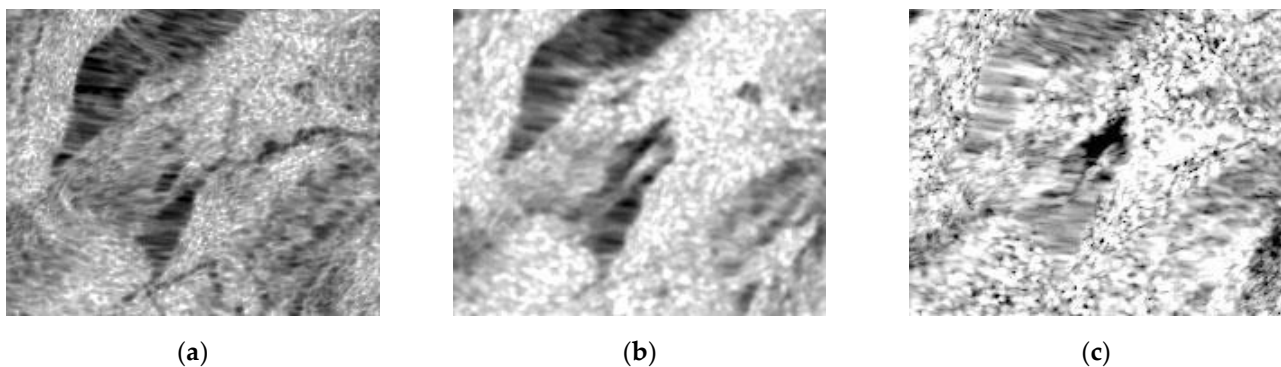


Figure 5.
(a) Sentinel 1 image for March 25, 2024; (b) Sentinel 1 image for April 18, 2024; (c) difference between Sentinel 1 images for the territory of Zailiysky Alatau.

The derived avalanche polygons were overlaid on high-resolution optical imagery and topographic maps to assess their spatial distribution and relationship to terrain features. We utilized PlanetScope satellite imagery (Figure 6a) to validate our avalanche mapping results by comparing avalanche occurrences, as identified by our Sentinel-1-based methodology, with independent observations from optical data [38]. False color composites were created using Blue, Green, and NIR channels at a resolution of 3 meters, and the boundaries of the detected avalanche accumulation zones were overlaid with our results. Furthermore, Sentinel-2 imagery (Figure 6b) available at a spatial resolution of 10m was also utilized to examine spectral signatures of avalanche deposits and differentiate them from other surface features. These images provided a visual reference for confirming the presence or absence of avalanches in specific locations, allowing us to assess the accuracy of our mapping results. Through this comparison, we were able to identify areas where avalanches were correctly detected, as well as instances of false positives or false negatives. By integrating multi-source data and validation techniques, we were able to evaluate the effectiveness and reliability of the Sentinel-1 SAR change detection method for avalanche mapping in the Northern Tien Shan.

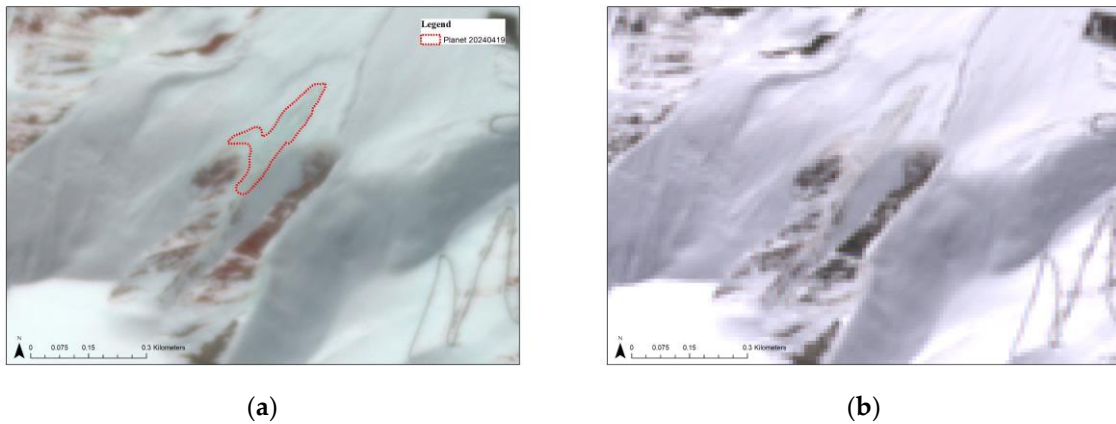


Figure 6. Avalanche identification on optical imagery using expert interpretation. (a) Planet image (acquisition date 19.04.2024), (b) Sentinel 2 image (acquisition date 19.04.2024).

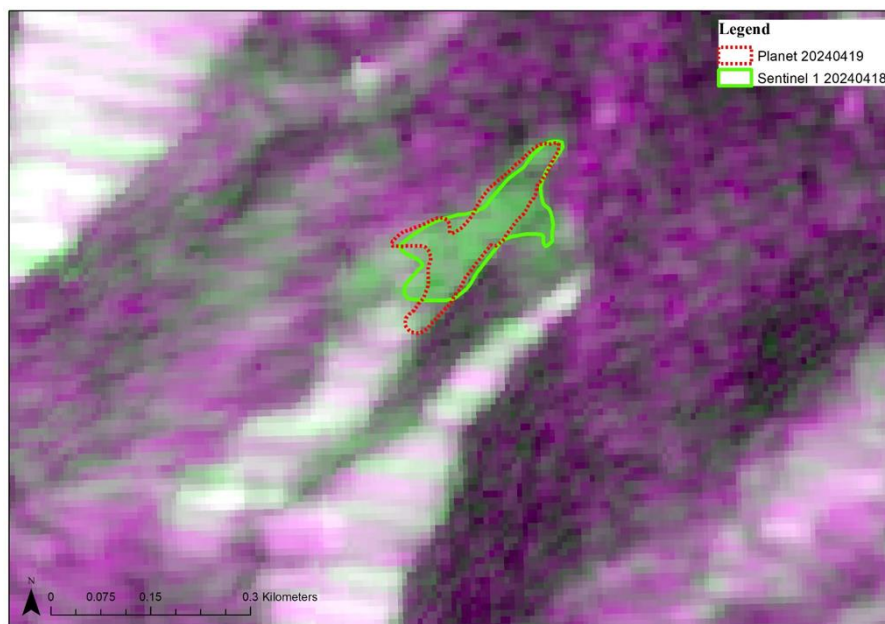


Figure 7. This is a figure. Schemes follow the same formatting.

Further, the avalanche contours presented in Figure 7, derived from both optical and radar data, the analysis demonstrate a general agreement when overlaid on an RGB composite generated from pre- and post-avalanche Sentinel-1 images. The green color indicates the changes that occurred between the acquisitions. Discrepancies are primarily attributed to differences in the acquisition geometry of the satellites and variations in their spatial resolution. These inconsistencies arise from the unique observation perspectives of each sensor, coupled with the differing resolutions at which they capture surface details. Additionally, temporal variations between the acquisitions of optical and radar images may contribute to these discrepancies, as changes in snow cover or avalanche debris extent may occur between the two acquisition times. Overall, the results of the study demonstrate the potential of Sentinel-1 SAR data for mapping snow avalanches in the Northern Tien Shan [39].

In our study, we explored the application of change detection algorithms to multi-temporal SAR data for the identification and mapping of snow avalanches in the Northern Tien Shan mountains. We utilized Sentinel-1 data,

benefiting from its high temporal resolution and sensitivity to surface changes, to detect alterations in backscatter intensity indicative of avalanche activity. Furthermore, we utilized decision tree classifiers to delineate the avalanche/non-avalanche boundaries by using various terrain parameters. To enhance the accuracy and reliability of our avalanche mapping results, we integrated multi-source data, including optical imagery and topographic data, and employed rigorous validation techniques. Thus, this approach not only automates the extraction of information from remote sensing data but also enhances the accuracy and reliability of avalanche mapping results.

The utilization of SAR data enables the detection of surface changes independent of weather conditions or solar illumination, making it particularly suitable for avalanche monitoring in regions prone to cloud cover or experiencing frequent periods of darkness. These performance advantages of SAR imagery over optical systems are particularly valuable in the remote and rugged terrain of the Tien Shan mountains, where timely and accurate information on avalanche occurrences is crucial for risk management and mitigation efforts. The continuous monitoring enabled by Sentinel-1 allows for tracking avalanche activity and identifying high-risk areas, contributing to improved hazard assessments and mitigation strategies [40]. By exploiting the spatial and temporal coverage offered by Sentinel-1, it is possible to map the entire Alps every 6 days, providing valuable information for avalanche monitoring and risk management [41]. The potential of Sentinel-1 data for mapping avalanche deposits on glaciers has been demonstrated, enabling the identification of avalanche hotspots and the quantification of avalanche activity across different regions [17]. SAR sensors, such as Sentinel-1, offer the advantage of acquiring data regardless of weather conditions or daylight, making them particularly suitable for avalanche monitoring in remote and inaccessible areas [40]. The high spatial resolution of SAR imagery allows for detailed mapping of avalanche debris and identification of avalanche paths, providing valuable information for hazard assessment and mitigation planning [42]. Improvements in radar technologies, data processing techniques, and sensor performance have expanded the application of SAR technology for slope monitoring and early warning systems [43]. Indeed, progress in differential Synthetic Aperture Radar interferometry has recently attracted much attention from researchers and practitioners involved in landslide monitoring and hazard assessment [44]. This technique has proven to be valid and reliable for measuring multitemporal land deformation on the Earth's surface by investigating point-like radar targets during acquisition time [45].

Several studies have demonstrated the effectiveness of using SAR data for detecting and mapping snow avalanches, particularly in mountainous regions where optical sensors may be limited by cloud cover or vegetation cover [41, 46] utilized multitemporal and multi-orbital radar images from TerraSAR-X and Sentinel-1 satellites to automatically detect and map avalanches in complex terrain in central Switzerland. Similarly, Bianchi and Grahn [18] demonstrated the effectiveness of Sentinel-1 data in combination with deep learning techniques for avalanche segmentation. Our study corroborates previous research, demonstrating the potential of Sentinel-1 SAR data for mapping snow avalanches in the Northern Tien Shan [47-50]. These studies contribute to enhancing our understanding of avalanche dynamics and improving the accuracy of avalanche hazard assessments. Furthermore, the integration of terrain data, such as slope, aspect, and elevation, with SAR-derived avalanche maps can provide valuable insights into the spatial distribution and triggering mechanisms of avalanches. Therefore, by leveraging the capabilities of Sentinel-1 SAR data and advanced change detection techniques, it is possible to map and monitor snow avalanches in high mountainous areas with high accuracy and efficiency [51].

Despite the effectiveness of Sentinel-1 SAR data for mapping snow avalanches, several limitations need to be considered. One limitation is the potential for misclassification of other surface changes, such as snowmelt or vegetation growth, as avalanches, particularly in areas with complex topography or heterogeneous land cover [52]. This can be addressed by incorporating additional data sources, such as optical imagery or LiDAR data, to better discriminate between different types of surface changes. Another limitation is the sensitivity of SAR backscatter to snow wetness, which can affect the accuracy of avalanche detection, especially during periods of rapid snowmelt [53]. Despite these limitations, the advantages of Sentinel-1 SAR data, including its high temporal resolution, all-weather imaging capabilities, and sensitivity to surface changes, make it a valuable tool for mapping and monitoring snow avalanches in the Northern Tien Shan and other mountainous regions [54].

Recent advancements in machine learning and deep learning have provided opportunities for automated analysis of large remote sensing datasets for avalanche detection and delineation [55, 56]. Indeed, deep learning systems can continuously learn and improve their predictive capabilities, adapting to new data and changing environmental conditions [57]. These technologies can also facilitate the integration of diverse datasets, including SAR imagery, optical imagery, terrain data, and meteorological data, to improve the accuracy and reliability of avalanche mapping. Machine learning algorithms have shown great promise in landslide and debris flow hazard analysis in several regions, offering possibilities for improving the accuracy and efficiency of geological hazard susceptibility evaluation [58]. Furthermore, the utilization of X and L band SAR images offers valuable data for terrain and land cover characterization, which can be useful in avalanche mapping [59, 60]. Fusing multi-source data can provide complementary information and improve the overall performance of avalanche detection and monitoring systems. Therefore, recent advances in remote sensing technologies combined with artificial intelligence, machine learning, and deep learning algorithms have high efficiency in avalanche monitoring and hazard mapping [61].

5. Conclusions

This study demonstrates the effectiveness of Sentinel-1 SAR data for mapping snow avalanches in the challenging terrain of the Northern Tien Shan. By leveraging the all-weather imaging capabilities and high temporal resolution of Sentinel-1, we have shown that it is possible to map and monitor avalanche activity with high accuracy and efficiency.

We acknowledge that there are limitations to using Sentinel-1 SAR data, such as the potential for misclassification due to snowmelt or vegetation changes. However, these limitations can be mitigated by incorporating additional data sources and advanced machine learning techniques. Recent advancements in deep learning offer promising avenues for automated analysis of remote sensing datasets and the integration of multi-source data, which can further improve the accuracy and reliability of avalanche mapping.

The continuous monitoring enabled by Sentinel-1 provides valuable information for risk management and mitigation efforts in avalanche-prone areas. By exploiting the spatial and temporal coverage offered by Sentinel-1, it is possible to track avalanche activity and identify high-risk zones. This contributes to improved hazard assessments and the development of more effective mitigation strategies.

In conclusion, this study highlights the significant potential of Sentinel-1 SAR data for avalanche monitoring and hazard mapping. The integration of SAR data with advanced data processing techniques and machine learning algorithms offers a powerful approach for understanding avalanche dynamics and improving the precision of avalanche hazard assessments. Future research should focus on refining these techniques and exploring the integration of additional data sources to further enhance the accuracy and reliability of avalanche mapping in complex terrain.

References

- [1] R. Ramirez, R. E. Abdullah, W. Jang, S.-K. Choi, and T.-H. Kwon, "Satellite-based monitoring of an open-pit mining site using Sentinel-1 advanced radar interferometry: A case study of the December 21, 2020, landslide in Toledo City, Philippines," in *E3S Web of Conferences (Vol. 415, p. 05020)*. EDP Sciences, 2023.
- [2] L. Liu, Y. Ma, N. Yao, and W. Ma, "Diagnostic analysis of a regional heavy snowfall event over the Tibetan Plateau using NCEP reanalysis data and WRF," *Climate Dynamics*, vol. 56, pp. 2451-2467, 2021. <https://doi.org/10.1007/s00382-020-05598-4>
- [3] L. Wang, M. Wang, X. Hung, and Z. Feng, "Research on LiDAR technology in early identification of geo-hazards in alpine loess areas," in *IOP Conference Series: Earth and Environmental Science (Vol. 570, No. 4, p. 042044)*. IOP Publishing, 2020.
- [4] S. Blumberg, "Climate change could Trigger More landslides in high mountain Asia," 2025. <https://www.nasa.gov/feature/goddard/2020/climate-change-could-trigger-more-landslides-in-high-mountain-asia/>. [Accessed 9 July 2025]
- [5] H. Wang *et al.*, "Disaster effects of climate change in High Mountain Asia: State of art and scientific challenges," *Advances in Climate Change Research*, vol. 15, no. 3, pp. 367-389, 2024. <https://doi.org/10.1016/j.accre.2024.06.003>
- [6] F. Guzzetti, A. C. Mondini, M. Cardinali, F. Fiorucci, M. Santangelo, and K.-T. Chang, "Landslide inventory maps: New tools for an old problem," *Earth-Science Reviews*, vol. 112, no. 1-2, pp. 42-66, 2012. <https://doi.org/10.1016/j.earscirev.2012.02.001>
- [7] M. Heck, C. Hammer, A. van Herwijnen, J. Schweizer, and D. Fäh, "Automatic detection of snow avalanches in continuous seismic data using hidden Markov models," *Natural Hazards and Earth System Sciences*, vol. 18, no. 1, pp. 383-396, 2018. <https://doi.org/10.5194/nhess-18-383-2018>
- [8] J. Schweizer, C. Mitterer, F. Techel, A. Stoffel, and B. Reuter, "On the relation between avalanche occurrence and avalanche danger level," *The Cryosphere*, vol. 14, no. 2, pp. 737-750, 2020. <https://doi.org/10.5194/tc-14-737-2020>
- [9] M. Eckerstorfer, H. Vickers, E. Malnes, and J. Grahn, "Near-real time automatic snow avalanche activity monitoring system using Sentinel-1 SAR data in Norway," *Remote Sensing*, vol. 11, no. 23, p. 2863, 2019. <https://doi.org/10.3390/rs11232863>
- [10] J. Liu *et al.*, "A study on avalanche-triggering factors and activity characteristics in Aexiangou, West Tianshan Mountains, China," *Atmosphere*, vol. 14, no. 9, p. 1439, 2023. <https://doi.org/10.3390/atmos14091439>
- [11] D. Stead, D. Donati, A. Wolter, and M. Sturzenegger, "Application of remote sensing to the investigation of rock slopes: Experience gained and lessons learned," *ISPRS International Journal of Geo-Information*, vol. 8, no. 7, p. 296, 2019. <https://doi.org/10.3390/ijgi8070296>
- [12] R. Macciotta and M. T. Hendry, "Remote sensing applications for landslide monitoring and investigation in western Canada," *Remote Sensing*, vol. 13, no. 3, p. 366, 2021. <https://doi.org/10.3390/rs13030366>
- [13] R. L. Ray, M. Lazzari, and T. Olutimehin, "Remote sensing approaches and related techniques to map and study landslides," *Landslides-Investig. Monit.*, vol. 2, pp. 1-25, 2020.
- [14] C. Vanneschi, M. Eyre, M. Francioni, and J. Coggan, "The use of remote sensing techniques for monitoring and characterization of slope instability," *Procedia Engineering*, vol. 191, pp. 150-157, 2017. <https://doi.org/10.1016/j.proeng.2017.05.166>
- [15] E. D. Hafner, F. Techel, S. Leinss, and Y. Bühler, "Mapping avalanches with satellites—evaluation of performance and completeness," *The Cryosphere*, vol. 15, no. 2, pp. 983-1004, 2021. <https://doi.org/10.5194/tc-15-983-2021>
- [16] J. Sykes, P. Haegeli, and Y. Bühler, "Automated snow avalanche release area delineation in data-sparse, remote, and forested regions," *Natural Hazards and Earth System Sciences*, vol. 22, no. 10, pp. 3247-3270, 2022. <https://doi.org/10.5194/nhess-22-3247-2022>
- [17] M. Kneib *et al.*, "Mapping and characterization of avalanches on mountain glaciers with Sentinel-1 satellite imagery," *The Cryosphere*, vol. 18, no. 6, pp. 2809-2830, 2024. <https://doi.org/10.5194/tc-18-2809-2024>
- [18] F. M. Bianchi and J. Grahn, "Monitoring snow avalanches from SAR data with deep learning," *arXiv preprint arXiv:2502.18157*, 2025. <https://doi.org/10.48550/ARXIV.2502.18157>
- [19] M. Lato, R. Frauenfelder, and Y. Bühler, "Automated detection of snow avalanche deposits: Segmentation and classification of optical remote sensing imagery," *Natural Hazards and Earth System Sciences*, vol. 12, no. 9, pp. 2893-2906, 2012. <https://doi.org/10.5194/nhess-12-2893-2012>
- [20] A. Caiserman, R. C. Sidle, and D. R. Gurung, "Snow Avalanche Frequency Estimation (SAFE): 32 years of remote hazard monitoring in Afghanistan," *The Cryosphere Discussions*, vol. 2022, pp. 1-26, 2022.
- [21] S. S. Ray, S. K. Singh, and S. Mamatha, "Establishing an operational system for assessment and forecasting the impact of extreme weather events on crop production," *Mausam*, vol. 67, no. 1, pp. 289-296, 2016. <https://doi.org/10.54302/mausam.v67i1.1230>

- [22] J. Wan *et al.*, "Refocusing of ground moving targets with Doppler ambiguity using keystone transform and modified second-order keystone transform for synthetic aperture radar," *Remote Sensing*, vol. 13, no. 2, p. 177, 2021. <https://doi.org/10.3390/rs13020177>
- [23] A. L. Handwerger, S. Y. Jones, M.-H. Huang, P. Amatya, H. R. Kerner, and D. B. Kirschbaum, "Rapid landslide identification using synthetic aperture radar amplitude change detection on the Google Earth engine," *Natural Hazards and Earth System Sciences Discussions*, vol. 2020, pp. 1-24, 2020.
- [24] A. Chigrinets, K. Duskayev, L. Mazur, L. Y. Chigrinets, S. Akhmetova, and A. Mussina, "Evaluation and dynamics of the glacial runoff of the rivers of the Ile Alatau northern slope in the context of global warming," *International Journal of Engineering Research and Technology*, vol. 13, no. 3, pp. 419-426, 2020.
- [25] K. Mukhtar, "The impact of climate change on the seismic vulnerability of the megalopolis of Almaty," *International Journal of Hydrology*, vol. 3, no. 1, pp. 52-56, 2019. <https://doi.org/10.15406/ijh.2019.03.00162>
- [26] K. Korzeniowska, Y. Bühler, M. Marty, and O. Korup, "Regional snow-avalanche detection using object-based image analysis of near-infrared aerial imagery," *Natural Hazards and Earth System Sciences*, vol. 17, no. 10, pp. 1823-1836, 2017. <https://doi.org/10.5194/nhess-17-1823-2017>
- [27] Q. Han and Z. Niu, "Construction of the long-term global surface water extent dataset based on water-NDVI spatio-temporal parameter set," *Remote Sensing*, vol. 12, no. 17, p. 2675, 2020. <https://doi.org/10.3390/rs12172675>
- [28] E. R. DeLancey, J. Kariyeva, J. T. Bried, and J. N. Hird, "Large-scale probabilistic identification of boreal peatlands using Google Earth Engine, open-access satellite data, and machine learning," *PLoS One*, vol. 14, no. 6, p. e0218165, 2019. <https://doi.org/10.1371/journal.pone.0218165>
- [29] D. Amitrano *et al.*, "Earth environmental monitoring using multi-temporal synthetic aperture radar: A critical review of selected applications," *Remote Sensing*, vol. 13, no. 4, p. 604, 2021. <https://doi.org/10.3390/rs13040604>
- [30] M. A. Iqbal, A. Anghel, and M. Datcu, "Doppler centroid estimation for ocean surface current retrieval from Sentinel-1 SAR data," in *2021 18th European Radar Conference (EuRAD) (pp. 429-432)*. IEEE, 2022.
- [31] Y. Cai, X. Li, M. Zhang, and H. Lin, "Mapping wetland using the object-based stacked generalization method based on multi-temporal optical and SAR data," *International Journal of Applied Earth Observation and Geoinformation*, vol. 92, p. 102164, 2020. <https://doi.org/10.1016/j.jag.2020.102164>
- [32] S. Hong, H. Jang, N. Kim, and H.-G. Sohn, "Water area extraction using RADARSAT SAR imagery combined with landsat imagery and terrain information," *Sensors*, vol. 15, no. 3, pp. 6652-6667, 2015. <https://doi.org/10.3390/s150306652>
- [33] P. Nakmuenwai, F. Yamazaki, and W. Liu, "Automated extraction of inundated areas from multi-temporal dual-polarization RADARSAT-2 images of the 2011 central Thailand flood," *Remote Sensing*, vol. 9, no. 1, p. 78, 2017. <https://doi.org/10.3390/rs9010078>
- [34] N. Parihar, A. Das, V. Rathore, M. Nathawat, and S. Mohan, "Analysis of L-band SAR backscatter and coherence for delineation of land-use/land-cover," *International Journal of Remote Sensing*, Vol. 35, no. 18, pp. 6781-6798, 2014. <https://doi.org/10.1080/01431161.2014.965282>
- [35] F. Raspini *et al.*, "Continuous, semi-automatic monitoring of ground deformation using Sentinel-1 satellites," *Scientific Reports*, vol. 8, p. 7253, 2018. <https://doi.org/10.1038/s41598-018-25369-w>
- [36] J. Yang *et al.*, "Automatic detection of regional snow avalanches with scattering and interference of C-band SAR Data," *Remote Sensing*, vol. 12, no. 17, p. 2781, 2020. <https://doi.org/10.3390/rs12172781>
- [37] X. Zhang, H. Su, C. Zhang, X. Gu, X. Tan, and P. M. Atkinson, "Robust unsupervised small area change detection from SAR imagery using deep learning," *ISPRS Journal of Photogrammetry and Remote Sensing*, vol. 173, pp. 79-94, 2021. <https://doi.org/10.1016/j.isprsjprs.2021.01.004>
- [38] E. D. Hafner, P. Barton, R. C. Daudt, J. D. Wegner, K. Schindler, and Y. Bühler, "Automated avalanche mapping from SPOT 6/7 satellite imagery: results, evaluation, potential and limitations," *The Cryosphere Discussions*, vol. 16, no. 9, pp. 3517-3530, 2022. <https://doi.org/10.5194/tc-16-3517-2022>
- [39] G. Forkuor, T. Ullmann, and M. Griesbeck, "Mapping and monitoring small-scale mining activities in Ghana using Sentinel-1 Time Series (2015-2019)," *Remote Sensing*, vol. 12, no. 6, p. 911, 2020. <https://doi.org/10.3390/rs12060911>
- [40] H. Vickers, M. Eckerstorfer, E. Malnes, Y. Larsen, and H. Hindberg, "A method for automated snow avalanche debris detection through use of synthetic aperture radar (SAR) imaging," *Earth and Space Science*, vol. 3, no. 11, pp. 446-462, 2016. <https://doi.org/10.1002/2016EA000168>
- [41] S. Leinss, R. Wicki, S. Holenstein, S. Baffelli, and Y. Bühler, "Snow avalanche detection and mapping in multitemporal and multiorbital radar images from TerraSAR-X and Sentinel-1," *Natural Hazards and Earth System Sciences*, vol. 20, no. 6, pp. 1783-1803, 2020. <https://doi.org/10.5194/nhess-20-1783-2020>
- [42] W. Sun, Q. Wang, W. Huang, C. Fan, and Y. Dai, "Vector current measurement using Doppler scatterometry with optimally selected observation azimuths," *Remote Sensing*, vol. 13, no. 21, p. 4263, 2021. <https://doi.org/10.3390/rs13214263>
- [43] C. Atzeni, M. Barla, M. Pieraccini, and F. Antolini, "Early warning monitoring of natural and engineered slopes with ground-based synthetic-aperture radar," *Rock Mechanics and Rock Engineering*, vol. 48, pp. 235-246, 2015. <https://doi.org/10.1007/s00603-014-0554-4>
- [44] C. Colesanti and J. Wasowski, "Investigating landslides with space-borne Synthetic Aperture Radar (SAR) interferometry," *Engineering Geology*, vol. 88, no. 3-4, pp. 173-199, 2006. <https://doi.org/10.1016/j.enggeo.2006.09.013>
- [45] P. Razi, J. T. S. Sumantyo, D. Perissin, and H. Kuze, "Long-term land deformation monitoring using Quasi-Persistent Scatterer (Q-PS) technique observed by sentinel-1A: Case Study Kelok Sembilan," *Advances in Remote Sensing*, vol. 7, pp. 277-289, 2018. <https://doi.org/10.4236/ars.2018.74019>
- [46] S. K. Roy, A. Deria, D. Hong, B. Rasti, A. Plaza, and J. Chansussot, "Multimodal fusion transformer for remote sensing image classification," *IEEE Transactions on Geoscience and Remote Sensing*, vol. 61, pp. 1-20, 2023. <https://doi.org/10.1109/TGRS.2023.3286826>
- [47] S.-J. Lee, H.-S. Yun, and T.-Y. Kim, "Monitoring of high-speed railway ground deformation using interferometric synthetic aperture radar image analysis," *Applied Sciences*, vol. 15, no. 8, p. 4318, 2025. <https://doi.org/10.3390/app15084318>
- [48] E. Psomiadis, M. Diakakis, and K. X. Soulis, "Combining SAR and optical earth observation with hydraulic simulation for flood mapping and impact assessment," *Remote Sensing*, vol. 12, no. 23, p. 3980, 2020. <https://doi.org/10.3390/rs12233980>

- [49] K. K. Singh *et al.*, "Detection and mapping of snow avalanche debris from Western Himalaya, India using remote sensing satellite images," *Geocarto International*, vol. 37, no. 9, pp. 2561-2579, 2022. <https://doi.org/10.1080/10106049.2020.1762762>
- [50] S. B. Wibowo *et al.*, "Spatio-temporal distribution of ground deformation due to 2018 lombok earthquake series," *Remote Sensing*, vol. 13, no. 11, p. 2222, 2021. <https://doi.org/10.3390/rs13112222>
- [51] A. Moreira, P. Prats-Iraola, M. Younis, G. Krieger, I. Hajnsek, and K. P. Papathanassiou, "A tutorial on synthetic aperture radar," *IEEE Geoscience and Remote Sensing Magazine*, vol. 1, no. 1, pp. 6-43, 2013. <https://doi.org/10.1109/MGRS.2013.2248301>
- [52] M. El Kamali, A. Abuelgasim, I. Papoutsis, C. Loupasakis, and C. Kontoes, "A reasoned bibliography on SAR interferometry applications and outlook on big interferometric data processing," *Remote Sensing Applications: Society and Environment*, vol. 19, p. 100358, 2020. <https://doi.org/10.1016/j.rsase.2020.100358>
- [53] R. C. Sharma, H. T. Nguyen, S. Gharechelou, X. Bai, L. V. Nguyen, and R. Tateishi, "Spectral features for the detection of land cover changes," *Journal of Geoscience and Environment Protection*, vol. 7, no. 05, pp. 81-93, 2019. <https://doi.org/10.4236/gep.2019.75009>
- [54] H. Lee and W. Li, "Geospatial artificial intelligence for satellite-based flood extent mapping: Concepts, advances, and future perspectives," *arXiv preprint arXiv:2504.02214*, 2025. <https://doi.org/10.48550/arXiv.2504.02214>
- [55] N. Prakash, A. Manconi, and S. Loew, "Mapping landslides on EO data: Performance of deep learning models vs. traditional machine learning models," *Remote Sensing*, vol. 12, no. 3, p. 346, 2020. <https://doi.org/10.3390/rs12030346>
- [56] R. A. Burange, H. K. Shinde, and O. Mutyalwar, "Landslide detection and mapping using deep learning across multi-source satellite data and geographic regions," *arXiv preprint arXiv:2507.01123*, 2025. <https://doi.org/10.2139/ssrn.5225437>
- [57] Q. Zhang and T. Wang, "Deep learning for exploring landslides with remote sensing and geo-environmental data: Frameworks, progress, challenges, and opportunities," *Remote Sensing*, vol. 16, no. 8, p. 1344, 2024. <https://doi.org/10.3390/rs16081344>
- [58] T. Qi, Y. Zhao, X. Meng, G. Chen, and T. Dijkstra, "Ai-based susceptibility analysis of shallow landslides induced by heavy rainfall in Tianshui, China," *Remote Sensing*, vol. 13, no. 9, p. 1819, 2021. <https://doi.org/10.3390/rs13091819>
- [59] A. Karpatne, I. Ebert-Uphoff, S. Ravela, H. A. Babaie, and V. Kumar, "Machine learning for the geosciences: Challenges and opportunities," *arXiv*, 2017. <https://doi.org/10.48550/arxiv.1711.04708>
- [60] J. Zhang, M. Yang, N. Dong, and Y. Wang, "Machine-learning-based ensemble prediction of the snow water equivalent in the Upper Yalong River Basin," *Sustainability*, vol. 17, no. 9, p. 3779, 2025. <https://doi.org/10.3390/su17093779>
- [61] S. Akosah, I. Gratchev, D.-H. Kim, and S.-Y. Ohn, "Application of artificial intelligence and remote sensing for landslide detection and prediction: systematic review," *Remote Sensing*, vol. 16, no. 16, p. 2947, 2024. <https://doi.org/10.3390/rs16162947>